

Electron-spin dynamics in Mn-doped GaAs using time-resolved magneto-optical techniques

I. A. Akimov,^{1,2} R. I. Dzhioev,² V. L. Korenev,² Yu. G. Kusrayev,² E. A. Zhukov,³ D. R. Yakovlev,^{1,2} and M. Bayer¹

¹*Experimentelle Physik II, Technische Universität Dortmund, 44221 Dortmund, Germany*

²*A.F. Ioffe Physical-Technical Institute, Russian Academy of Sciences, 194021 St. Petersburg, Russia*

³*Faculty of Physics, M. V. Lomonosov Moscow State University, 119992 Moscow, Russia*

(Received 23 July 2009; published 12 August 2009)

We study the electron-spin dynamics in *p*-type GaAs doped with magnetic Mn acceptors by means of time-resolved pump-probe and photoluminescence techniques. Measurements in transverse magnetic fields show a long spin-relaxation time of 20 ns that can be uniquely related to electrons. Application of weak longitudinal magnetic fields above 100 mT extends the spin-relaxation times up to microseconds which is explained by suppression of the Bir-Aronov-Pikus spin relaxation for the electron on the Mn acceptor.

DOI: [10.1103/PhysRevB.80.081203](https://doi.org/10.1103/PhysRevB.80.081203)

PACS number(s): 78.55.Cr, 71.35.Ji, 75.50.Pp, 78.47.-p

The spin dynamics in semiconductors have attracted strong interest for several decades and nowadays are in the focus of attention for spin electronics and quantum information applications.¹⁻⁴ Materials with long spin lifetimes and efficient mechanisms for controlling spin relaxation, e.g., by weak magnetic fields, are required for these purposes. A large amount of work has been mainly done on *n*-type GaAs, where spin-relaxation times in the range of 100 ns have been observed.⁵⁻⁷ Long spin-relaxation times in the order of microseconds have been also observed in strong longitudinal magnetic fields $B > 2$ T.^{8,9}

In *p*-type GaAs fast electron-spin relaxation on the order of several ns or shorter takes place due to electron-hole exchange interaction known as Bir-Aronov-Pikus (BAP) mechanism.¹⁰ For this reason *p*-type structures were out of the focus until recent publications of Astakhov *et al.*¹¹ in bulk and Myers *et al.*¹² in quantum wells doped with magnetic Mn acceptors. Both groups reported surprisingly long spin memory in *p*-type GaAs:Mn evaluated from Hanle measurements. However the origin of this effect was interpreted differently. In Ref. 11 it was attributed to long-lived electron-spin memory, while in Ref. 12 to the spin dynamics of Mn acceptors. This difference is surprising as the hole localization at the acceptor (~ 1 nm) is smaller than the quantum well width so that A_{Mn}^0 should mainly keep its bulk properties. The problem originates from the separation of contributions of the electron and magnetic acceptor spin orientations into the polarization of the optical $e-A_{Mn}^0$ transition, being present in any Mn-doped GaAs structure bulk, quantum well, wire, or dot. In previous publications^{11,12} the authors used indirect measurements such as Hanle effect under cw excitation, where the g factor of the oriented particles is unknown, as well as time-resolved Kerr rotation, where the probe beam energy does not necessarily corresponds to the energy of the transition contributing to the detected signal. Therefore both methods cannot unambiguously solve the aforementioned problem.

In this Rapid Communication we report on direct measurement of the spin dynamics based on polarization- and time-resolved studies of the photoluminescence (PL). This enables us to measure g factor, lifetime, and spin-relaxation time at the $e-A_{Mn}^0$ optical transition energy. From spin quantum beats with a frequency corresponding to the electron g factor we conclude that the long spin-relaxation time in bulk

GaAs:Mn is related to the electrons and not the magnetic acceptors. A rather weak longitudinal magnetic field B of about 100 mT stretches τ_S by a factor of 50 from 20 ns to 1 μ s, much longer than previously reported for spin-relaxation times in bulk GaAs subject to weak magnetic fields. This result is interpreted as suppression of the BAP spin-relaxation mechanism for the magnetic Mn acceptor. The data are consistent with time-resolved Faraday rotation measurements.

The investigated sample was grown by liquid phase epitaxy on a (001)-oriented GaAs substrate. The thickness of the GaAs:Mn layer is 36 μ m and the concentration of Mn acceptors is 8×10^{17} cm⁻³. The acceptors are partially compensated by residual donors.¹¹ The PL spectrum of this sample in Fig. 1(a) consists of the exciton (X) and donor-acceptor ($D^0-A_{Mn}^0$) emission lines.

For Faraday (Kerr) rotation measurements two synchronized mode-locked Ti:Sa lasers operating at independently variable wavelengths were used as sources of pump and probe pulses. The lasers emitted pulses with 1 ps duration and 2 nm spectral width at a repetition frequency of 76 MHz. The sample was held in a split-coil cryostat for magnetic fields $B \leq 7$ T. The laser beams were directed along the sample growth axis (z axis) and the magnetic field was applied perpendicular to it, $\mathbf{B} \perp \mathbf{z}$ (Voigt geometry). To exclude dynamic nuclear polarization, the helicity of the pump beam was modulated with a photoelastic modulator at 50 kHz frequency. The rotation angle of the linearly polarized transmitted (reflected) probe pulse was homodyne detected with a balanced photodiode and a lock-in amplifier.

For time-resolved PL measurements we used a Ti:Sa laser combined with a pulse picker by which the pulse separation was extended to 1.3 μ s. The energy of the circularly polarized excitation photons was tuned to $\hbar\omega_{exc} = 1.56$ eV, slightly above the GaAs band gap. The sample was mounted in a He-bath cryostat and magnetic fields up to 0.2 T were applied in Voigt or Faraday geometry using an electromagnet. The PL signal was dispersed by a single monochromator with 6.28 nm/mm linear dispersion and detected with a streak camera allowing for a time resolution down to 50 ps. PL detection with either σ^+ or σ^- polarization after σ^+ excitation was selected by rotating a $\lambda/4$ plate with a subsequent Glan-Thomson prism. The degree of circular polarization was determined as $\rho_c = (I_+ - I_-)/(I_+ + I_-)$, where I_+ and I_- are

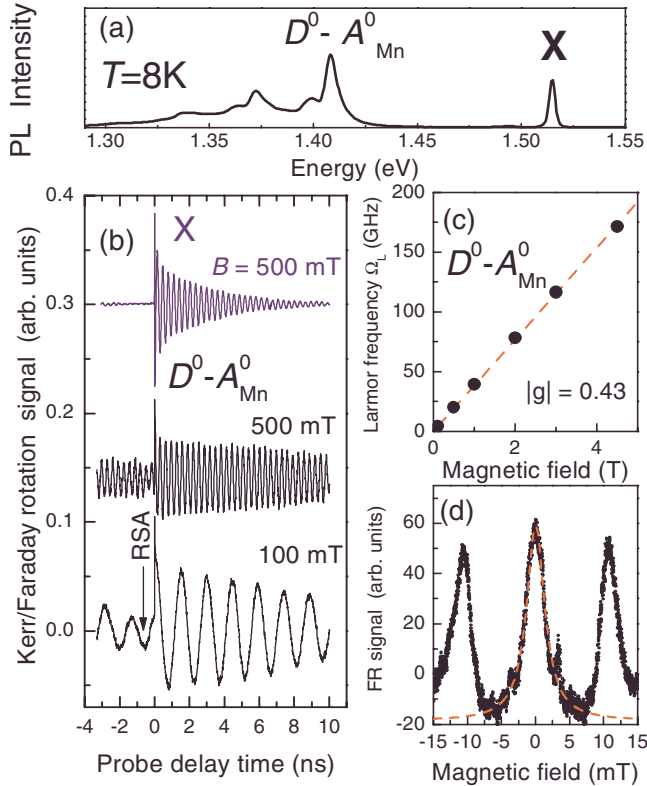


FIG. 1. (Color online) (a) PL spectrum of GaAs:Mn under moderate excitation with pulse power $P=1 \mu\text{J}/\text{cm}^2$. (b) Top: Kerr rotation at exciton resonance $\hbar\omega_{\text{pump}}=\hbar\omega_{\text{probe}}=1.516 \text{ eV}$ for degenerate pump probe. Mid and bottom: two-color FR with pump at 1.520 eV and probe at 1.406 eV. (c) Larmor frequency in FR vs magnetic field. Line is linear fit to the data. (d) Resonant spin amplification in FR measured for pump-probe pulse delay -640 ps [see arrow in (b)]. Dashed curve is Lorentzian fit of central peak.

the σ^+ and σ^- polarized PL intensities, respectively. For all experiments the temperature was kept at $T=8 \text{ K}$.

First, we discuss results of time-resolved Faraday (Kerr) rotation. The typical signals in Fig. 1(b) show oscillations with a decreasing amplitude with increasing delay between pump and probe. The signal is proportional to the time evolution of the z projection of the photoinduced average spin which can be well described by the form $\cos(\Omega_L t)\exp(-t/T_2^*)$. Here T_2^* is the dephasing time of the spin ensemble and $\Omega_L=g\mu_B B/\hbar$ is the Larmor frequency,¹³ where μ_B is the Bohr magneton and g is the g factor. The value of $|g|=0.43\pm 0.01$ as determined from a linear fit to the $\Omega_L(B)$ dependence measured for the $D^0-A_{Mn}^0$ transition [see Fig. 1(c)] is identical with the electron g factor in GaAs. This allows us to assign the measured signals to optically oriented electrons. The photogenerated holes rapidly lose their spin due to the complex valence-band structure and therefore give no contribution to the long-lived spin dynamics.¹ We do not find any evidence of a Mn-acceptor spin orientation, which would give rise to oscillations with frequencies corresponding to $g_{A^0}=2.74$ and $g_{A^-}=2.02$ for the neutral and ionized Mn acceptor, respectively.^{14,15}

For degenerate Kerr rotation, where the energies of pump $\hbar\omega_{\text{pump}}$ and probe $\hbar\omega_{\text{probe}}$ coincide, signal is detected only close to the exciton (X) resonance [upper curve in Fig. 1(b)],

decaying with the exciton lifetime $\tau_X=3 \text{ ns}$ (Ref. 16) and oscillating according to $|g|=0.43$. In two-color Faraday rotation (FR) the pump laser excites free carriers at the band edge of GaAs ($\hbar\omega_{\text{pump}}=1.520 \text{ eV}$), while the probe at the $D^0-A_{Mn}^0$ energy ($\hbar\omega_{\text{probe}}=1.406 \text{ eV}$) propagates through the sample without significant absorption. For weak magnetic fields $B\leq 500 \text{ mT}$ the signal decays on a much longer time scale compared to the exciton as one can see from the strong signal at negative delays. We measured its decay time T_2^* by the resonant spin amplification (RSA) technique,⁷ in which the FR signal was detected as function of magnetic field at a fixed negative delay of -640 ps [Fig. 1(d)]. The central RSA peak is fitted by a Lorentzian, whose half width at half maximum $B_{1/2}=1.6 \text{ mT}$ gives $T_2^*=\hbar/g\mu_B B_{1/2}\approx 17 \text{ ns}$. The dephasing rate in the limit of low magnetic fields $1/T_2^*$ corresponds to the inverse spin lifetime $1/T_S=1/\tau_S+1/\tau$, where τ is the electron lifetime. The long dephasing time of $T_2^*\approx 17 \text{ ns}$ indicates that the spin lifetime is related to long-lived electrons, which eventually recombine with acceptor bound holes. However the FR spectral dependence on the probe pulse energy does not allow to attribute the signal to a certain optical transition unambiguously, e.g., $e-A_{Mn}^0$, because the form of the signal remains the same for $1.4 < \hbar\omega_{\text{probe}} < 1.5 \text{ eV}$. In addition the spin lifetime T_S depends on both τ and τ_S , and for determining τ_S one needs to know τ .

Time-resolved measurements of the total PL intensity $I(t)=I_++I_-$ and polarization degree $\rho_c(t)$ allow us to determine both τ and τ_S exactly for the optical $e-A_{Mn}^0$ transition energy. The intensity is related to the population decay $I(t)\propto \exp(-t/\tau)$, while $\rho_c(t)=\rho_c(0)\exp(-t/\tau_S)$ gives direct access to the spin dynamics of oriented electrons. Moreover, in transverse magnetic field the carrier g factor can be determined from the oscillations of $\rho_c(t)$, similar to the pump-probe experiment.¹⁷ Transients measured at $B=0$ and 11 mT in Voigt geometry are shown in Fig. 2. From $I(t)$ and $\rho_c(t)$ at zero magnetic field we find $\tau=110 \text{ ns}$ and $\tau_S=23 \text{ ns}$. These values give $T_S=19 \text{ ns}$, which is in good agreement with the value obtained from FR. We do not observe a dependence of these times on excitation power up to a moderate pulse intensity $P=1 \mu\text{J}/\text{cm}^2$.

In transverse magnetic field we detect pronounced oscillations of the circular polarization degree [Fig. 2(b)], which can be well fitted by $\rho_c(t)=\rho_c(0)\cos(\Omega_L t)\exp(-t/\tau_S)$. The Larmor frequency dependence on magnetic field in the inset gives an electron g factor of $|g|=0.42\pm 0.02$. The initial electron spin is $S_z(0)=\rho_c(0)\approx 0.2$, which is close to the maximum value of 0.25.¹ In agreement with the FR, we therefore conclude from the PL data that the long-lived spin dependent signal is contributed solely by donor-bound electrons.

Further insight in the spin dynamics is obtained from experiments in Faraday geometry, where the electron-spin relaxation is typically suppressed with increasing magnetic field.¹ For GaAs:Mn we observe strong changes already in weak fields, see Fig. 3(a) and 3(b). The longitudinal electron-spin-relaxation time τ_S^* increases from 20 ns at zero field up to $1 \mu\text{s}$ at 140 mT, as shown by the magnetic fields dependence of τ_S^* in panel (b).

Before discussing the data let us consider the four main mechanisms responsible for electron-spin relaxation. Two of

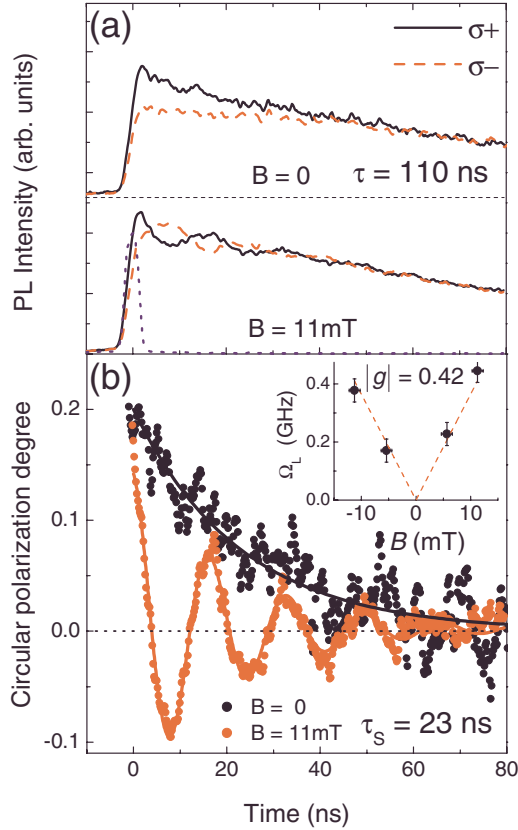


FIG. 2. (Color online) (a) PL transients of $D^0-A_{Mn}^0$ emission line under σ^+ excitation at 1.560 eV measured for σ^+ (solid line) and σ^- (dashed) polarization at $B=0$ and 11 mT in Voigt geometry. The laser apparatus function is shown by the dotted curve. (b) Time evolution of circular polarization degree. Solid lines are fits. Inset shows precession frequency Ω_L as function of magnetic field. Line is linear fit with $|g|=0.42 \pm 0.02$.

them related to spin-orbit interaction, the Elliot-Yafet and Dyakonov-Perel' mechanisms, are not relevant for our case since the electrons are bound to donors at low temperatures. The hyperfine interaction of the electron with nuclear spins can provide relaxation times in the microsecond range for donor concentrations of 10^{16} cm^{-3} (Ref. 18) and thus is much longer than the typical times due to electron exchange interaction with holes bound to acceptors. This Bir-Aronov-Pikus mechanism dominates in samples with acceptor concentrations exceeding 10^{17} cm^{-3} .¹⁰

The suppression of spin relaxation by a longitudinal magnetic field can be described in the motional averaging model by

$$\tau_S^* = \tau_S [1 + (B/B_c)^2]. \quad (1)$$

Here $B_c = \hbar / [(g_A^0 - g) \mu_B \tau_c]$ and τ_c is the correlation time during which the random field resulting in spin relaxation can be considered as constant.^{1,19} The regular change in the random field due to hole spin precession in the external field is taken into account through the neutral acceptor g factor g_A^0 in the expression for B_c . The spin-relaxation rate at zero magnetic field is given by

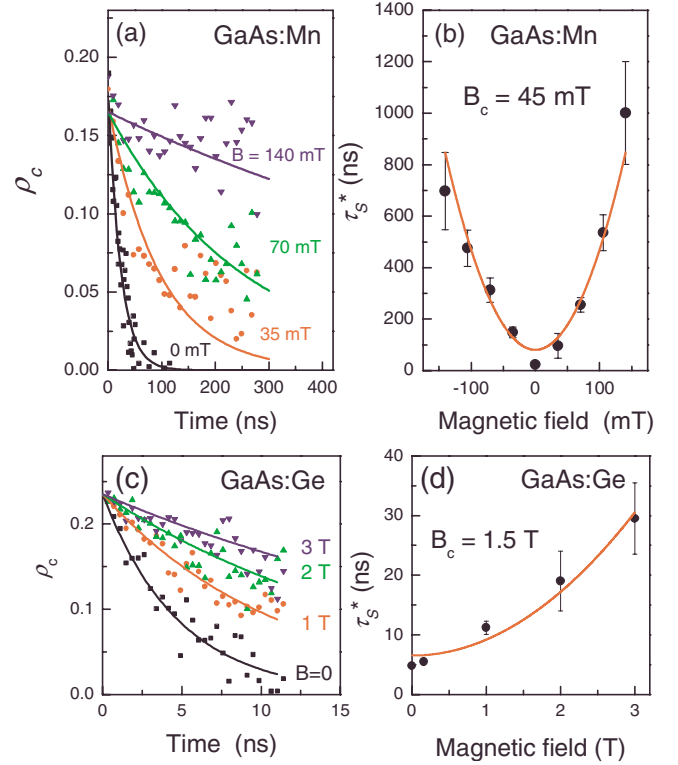


FIG. 3. (Color online) (a) Time-resolved circular polarization degree of $D^0-A_{Mn}^0$ emission line for different longitudinal magnetic fields at $P=0.2 \mu\text{J}/\text{cm}^2$. Lines are exponential fits. (b) Spin-relaxation time τ_S^* as function of magnetic field in Mn-doped sample. Line is fit with Eq. (1). (c) and (d) same as (a) and (b) for $D^0-A_{Ge}^0$ line in GaAs:Ge sample measured at $P=1 \mu\text{J}/\text{cm}^2$.

$$\frac{1}{\tau_S} = \frac{2}{3} \omega_f^2 \tau_c. \quad (2)$$

The rms value of the electron-spin precession frequency ω_f in the random field characterizes the field strength. The experimental data in Fig. 3(b) can be well fitted by Eq. (1), as shown by the solid line, except for the data point at $B=0$.²⁰ We find from this fit $\tau_S \approx 70 \text{ ns}$ and $B_c \approx 45 \text{ mT}$, which is close to the continuous-wave Hanle data for moderate pump intensities which give $\tau_S = 160 \text{ ns}$.¹¹ Assuming the acceptors are neutral, i.e., $g_A^0 - g = 3.16$, we find $\tau_c \approx 80 \text{ ps}$.

For comparison we have measured a typical p -type GaAs:Ge sample with comparable concentration of nonmagnetic Ge acceptors of $6 \times 10^{17} \text{ cm}^{-3}$ (lower panels in Fig. 3). The PL transients of the donor-acceptor emission line give a decay time $\tau \approx 3.3 \text{ ns}$. The PL circular polarization decays with $\tau_S = 4.7 \text{ ns}$ at $B=0$, showing no significant change for $B < 200 \text{ mT}$. With increasing field it increases, and τ_S^* reaches 30 ns at $B=3 \text{ T}$.²¹ A fit according to Eq. (1) gives $B_c \approx 1.5 \text{ T}$. With $g_A = 0.7$ for Ge,²² we find $\tau_c \approx 7 \text{ ps}$, which is significantly shorter than in Mn-doped GaAs. Using Eq. (2) we find that ω_f^2 is about 100 times larger in GaAs:Ge than in GaAs:Mn.

The exchange interaction energy between the electron spin \mathbf{S} and total magnetic moment of the neutral Mn acceptor \mathbf{F} is $H_S = -a_F (\mathbf{S} \cdot \mathbf{F})$, where a_F depends on the exchange constant $\Delta_{A_{Mn}^0}$ and the overlap of the electron and acceptor hole

wave functions.¹¹ The extension of the donor-bound electron given by the Bohr radius a_B is much larger than the Mn acceptor. Therefore the precession frequency of the electron spin in the effective magnetic field of the Mn acceptor, which is located at a distance R from the donor, is $\bar{\omega}_f = \Delta_{A_{Mn}}^0 \mathbf{F} \exp(-2R/a_B)/\hbar$. By averaging $\langle \dots \rangle$ over the donor-acceptor distances one obtains

$$\omega_f^2 = \frac{\Delta_{A_{Mn}}^2 F(F+1)}{\hbar^2} \left\langle \exp\left(-\frac{4R}{a_B}\right) \right\rangle. \quad (3)$$

The Mn-acceptor ground state corresponds to the antiparallel configuration of the hole and Mn spins with angular momentum $F=1$. It follows from Eq. (3) that ω_f^2 depends not only on the exchange constant $\Delta_{A_{Mn}}^0$ but also on the distribution of the impurities. In case of a nonmagnetic acceptor ω_f^2 is given by the same Eq. (3), the exchange constant $\Delta_{A_{Mn}}^0$ and momentum F , however, has to be substituted by the electron-hole exchange energy $\Delta_{A_{Ge}}^0$ and the total angular momentum of the hole $J=3/2$.¹⁹

As mentioned, ω_f^2 differs by two orders of magnitude in Ge- and Mn-doped samples. Two reasons may be responsible for its strong decrease in GaAs:Mn. The first is the antiferromagnetic coupling between the hole and Mn spins, which reduces $\Delta_{A_{Mn}}^0$ and F compared with the nonmagnetic Ge acceptor.^{11,23} The second is related to the larger average distance R between donors and acceptors in GaAs:Mn as compared to GaAs:Ge with similar doping concentration. This is

supported by a factor 30 difference in the emission decay times measured for the D^0 - A^0 transitions.

The correlation times τ_c also differ strongly in Ge- and Mn-doped samples. For electrons localized on shallow donors, τ_c is determined by either the electron-spin hopping time between donors or by the spin-relaxation time of the hole bound to an acceptor, whichever is the shorter one. For a donor concentration of 10^{16} cm^{-3} the electron hopping time is on the order of 10–100 ps.^{18,19} Therefore we conclude that the short correlation time of $\tau_c \approx 7$ ps in GaAs:Ge is mainly due to hole spin relaxation. In contrast, the long $\tau_c \approx 80$ ps in GaAs:Mn suggests that the spin relaxation of the Mn acceptor occurs on a time scale comparable or longer than the spin hopping time. The reason for this difference is the strong spin coupling of the hole with the Mn spin.

In conclusion we have shown that the long spin-relaxation time exceeding 20 ns in GaAs doped with Mn is related with electrons. The long correlation time leads to the small external magnetic fields required to suppress the Bir-Aronov-Pikus mechanism, which controls the spin dynamics of bound electrons. An important role plays also g factor of the hole bound to the acceptor which is almost four times larger in GaAs:Mn as compared with nonmagnetic GaAs. These features allow us to extend the electron-spin-relaxation time up to 1 μs in weak longitudinal magnetic fields in the 100 mT range.

The authors thank G. V. Astakhov for useful discussions. This work was supported by the Deutsche Forschungsgemeinschaft (Grant No. 436RUS113/958/0-1) and the Russian Foundation for Basic Research.

¹*Optical Orientation*, edited by F. Meyer and B. P. Zakharchenya (North-Holland, Amsterdam, 1984).

²*Semiconductor Spintronics and Quantum Computation*, edited by D. D. Awschalom, D. Loss, and N. Samarth (Springer-Verlag, Berlin, 2002).

³*Spin Physics in Semiconductors*, edited by M. I. Dyakonov (Springer-Verlag, Berlin, 2008).

⁴*Optical Orientation*, edited by Y. Kusrayev and G. Landwehr, special issue of *Semicond. Sci. Technol.* **23** (11) (2008).

⁵C. Weisbuch, Ph.D. thesis, University of Paris, 1977.

⁶R. I. Dzhiyev, B. P. Zakharchenya, V. L. Korenev, and M. N. Stepanova, *Phys. Solid State* **39**, 1765 (1997).

⁷J. M. Kikkawa and D. D. Awschalom, *Phys. Rev. Lett.* **80**, 4313 (1998).

⁸J. S. Colton, T. A. Kennedy, A. S. Bracker, and D. Gammon, *Phys. Rev. B* **69**, 121307(R) (2004).

⁹Kai-Mei C. Fu, W. Yeo, S. Clark, C. Santori, C. Stanley, M. C. Holland, and Y. Yamamoto, *Phys. Rev. B* **74**, 121304(R) (2006).

¹⁰G. I. Bir, A. G. Aronov, and G. E. Pikus, *Sov. Phys. JETP* **42**, 705 (1976).

¹¹G. V. Astakhov, R. I. Dzhiyev, K. V. Kavokin, V. L. Korenev, M. V. Lazarev, M. N. Tkachuk, Yu. G. Kusrayev, T. Kiessling, W. Ossau, and L. W. Molenkamp, *Phys. Rev. Lett.* **101**, 076602 (2008).

¹²R. C. Myers, M. H. Mikkelsen, J. M. Tang, A. C. Gossard, M. E. Flatte, and D. D. Awschalom, *Nature Mater.* **7**, 203 (2008).

¹³S. A. Crooker, D. D. Awschalom, J. J. Baumberg, F. Flack, and

N. Samarth, *Phys. Rev. B* **56**, 7574 (1997).

¹⁴J. Schneider, U. Kaufmann, W. Wilkening, M. Baeumler, and F. Köhl, *Phys. Rev. Lett.* **59**, 240 (1987).

¹⁵V. F. Sapega, T. Ruf, and M. Cardona, *Phys. Status Solidi B* **226**, 339 (2001).

¹⁶G. W. 't Hooft, W. A. J. A. van der Poel, L. W. Molenkamp, and C. T. Foxon, *Phys. Rev. B* **35**, 8281 (1987).

¹⁷A. P. Heberle, W. W. Rühle, and K. Ploog, *Phys. Rev. Lett.* **72**, 3887 (1994).

¹⁸R. I. Dzhiyev, K. V. Kavokin, V. L. Korenev, M. V. Lazarev, B. Ya. Meltser, M. N. Stepanova, B. P. Zakharchenya, D. Gammon, and D. S. Katzer, *Phys. Rev. B* **66**, 245204 (2002).

¹⁹M. I. Dyakonov and V. I. Perel', *Sov. Phys. JETP* **38**, 177 (1974).

²⁰The threefold reduction of τ_S from 70 to 23 ns at zero magnetic field cannot be related to dynamical nuclear polarization as the 20 ns time has been measured by pump-probe FR with modulated light polarization to suppress nuclear effects. No singularity of τ_S is observed for GaAs:Ge at zero field, indicating that the reduction is related to specifics of the magnetic Mn acceptor. The detailed study of this effect will be performed in future.

²¹For stronger magnetic fields we analyze the average of $\rho_c(t)$ measured in opposite field directions. This allows us to exclude effects related to carrier thermalization on the Zeeman sublevels.

²²V. F. Sapega, T. Ruf, M. Cardona, K. Ploog, E. L. Ivchenko, and D. N. Mirlin, *Phys. Rev. B* **50**, 2510 (1994).

²³C. Śliwa and T. Dietl, *Phys. Rev. B* **78**, 165205 (2008).